



Lignin-derived carbon-based solid acid catalyst for the conversion of *Pueraria* cellulose to lactic acid

Hui Kang · Jie Guo · Xiang-tong Gai · Jian He ·
Xian-wu Zhou · Ke Song

Received: 31 July 2023 / Accepted: 4 December 2023 / Published online: 18 December 2023
© The Author(s), under exclusive licence to Springer Nature B.V. 2023

Abstract Preparation of lactic acid (LaA) from waste biomass *Pueraria* cellulose by chemically catalyzed conversion is important for the realization of biomass waste resource utilization. In this study, lignin was used as raw material to prepare lignin-based carbonaceous support (LCSA) by one-step sulfonation and carbonization with chlorosulfonic acid. LCSA–Al_xZn_y, a lignin-based carbon solid acid

catalyst, was obtained by modifying the carbonaceous support with inexpensive and readily available Al and Zn chlorides. Through the use of SEM, BET, XRD, FT-IR and NH₃-TPD, the catalyst's physical as well as chemical characteristics were identified. In an aqueous solution, these catalysts were evaluated for the generation of LaA from *Pueraria* cellulose. LCSA–Al was identified as the optimal catalyst, subsequently, experimental conditions such as reaction time, reaction temperature, and catalyst dosage were studied and optimized. The results showed that at 160 °C, with 50 mg *Pueraria* cellulose, 50 mg catalyst, and 10 mL deionized water, the conversion rate of *Pueraria* cellulose was 53.7% and the highest LaA yield was 24.7% after 120 min of reaction. This research provides a new pathway for the preparation of chemicals from cellulose via multi-step tandem catalytic reactions.

Supplementary Information The online version contains supplementary material available at <https://doi.org/10.1007/s10570-023-05684-w>.

H. Kang · J. Guo · X. Gai · J. He · X. Zhou · K. Song
College of Chemistry and Chemical Engineering, Jishou University, Jishou 416000, China
e-mail: 2021700422@stu.jsu.edu.cn

J. Guo
e-mail: guojie1981@jsu.edu.cn

X. Gai
e-mail: 2022700477@stu.jsu.edu.cn

J. He
e-mail: jianhelch@jsu.edu.cn

X. Zhou
e-mail: zhouxianwu@jsu.edu.cn

H. Kang · J. Guo · X. Gai · J. He · X. Zhou · K. Song (✉)
Key Laboratory of Hunan Forest Products and Chemical Industry Engineering, National and Local United Engineering Laboratory of Integrative Utilization Technology of *Eucommia Ulmoides*, Jishou University, Zhangjiajie 427000, China
e-mail: kesong@jsu.edu.cn

Keywords *Pueraria* cellulose · Lactic acid · Lignin · Solid acid · Catalytic conversion

Introduction

Converting inedible agricultural and forestry waste into profitable substances, fuels, as well as materials is a practical manner to solve environmental problems and promote the development of a circular economy. *Pueraria edulis* Pampan. is a dietary and curative plant (Guo et al. 2021), and after extracting its starch,

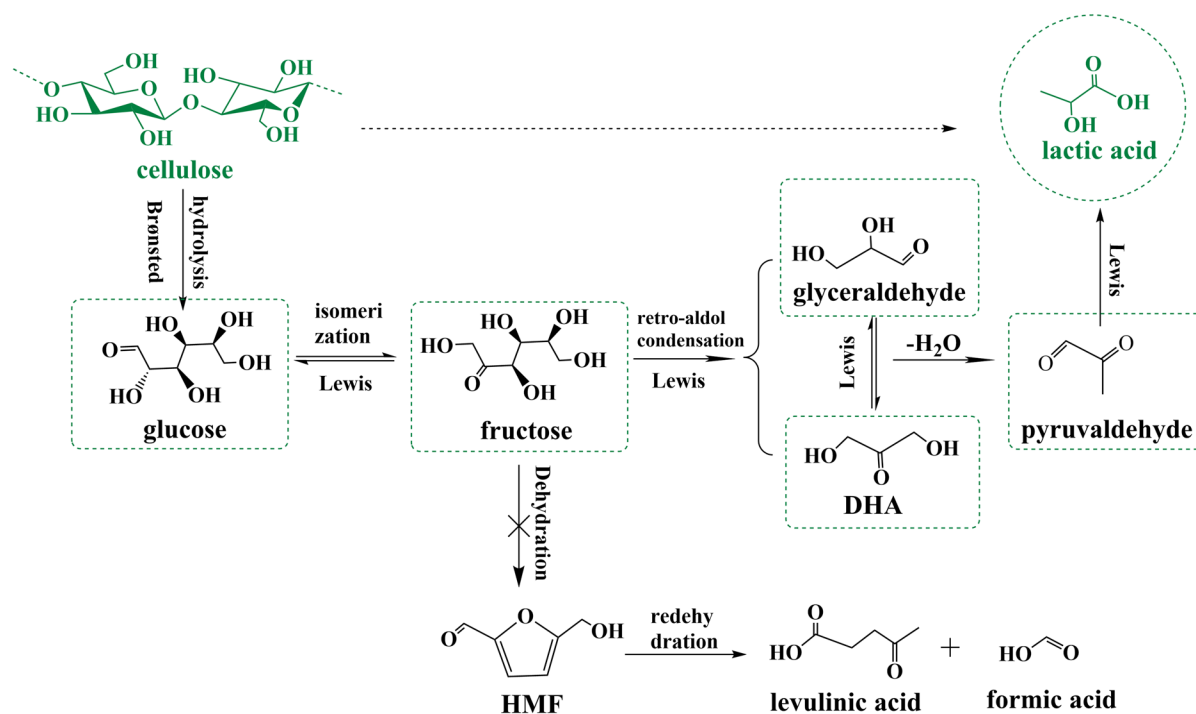
a large amount of *P. edulis* Pampan. residue is left. Landfilling or incinerating this residue would cause environmental pollution and waste of resources. However, *P. edulis* Pampan. residue has a cellulose content of 59% (Peng et al. 2022), which can be hydrolyzed to produce glucose (Wu et al. 2020) and subsequently be transformed into a variety of platform chemicals, including fructose (Marianou et al. 2016; Chen et al. 2020), HMF (Wei et al. 2022), levulinic acid (Chen et al. 2022) and Lactic acid (LaA) (Ye et al. 2021), among others. Within these, LaA is the primary monomer used in the synthesis of the biodegradable polymer polylactic acid. Finding an effective and ecologically friendly chemical conversion pathway for the production of LaA using cellulose, native biomass from *P. edulis* Pampan. residue, as raw material, is a crucial and challenging task.

A multifunctional-hydroxy carboxylic acid, LaA (2-hydroxypropionic acid) has a number of applications in the chemical, medicinal, and food various industries. As a component for producing green solvents or other bio-based compounds like acrylic acid, 2,3-pentanedione, and acetaldehyde, LaA has garnered significant study interest (SerranoRuiz et al. 2011; Dusselier et al. 2013; Deng et al. 2018a, 2018b). Currently, the production of LaA is mainly based on a bio-fermentation process, which involves the pre-treatment of biomass with acid or alkali. In addition, biological enzymes are highly sensitive to the working environment during fermentation, and strict control of the reaction medium's pH value is required, making the operation process complex (Dusselier et al. 2013; Castillo Martinez et al. 2013; Qureshi et al. 2017). Compared to traditional LaA production processes, designing a rational green and sustainable catalytic system for catalyzing the conversion of abundant biomass resources (such as cellulose biomass) into high value-added product LaA has important research significance (Wattanapaphawong et al. 2017).

Dihydroxyacetone (Dapsens et al. 2013; Feliczak-Guzik et al. 2018; Hossain et al. 2021; Rahaman et al. 2022), glycerol (Xu et al. 2013, 2022; Lu et al. 2016; Palacio et al. 2018), hexoses (glucose and fructose) (Zhao et al. 2018, 2021; Wang et al. 2021; Kupila et al. 2021), cellulose and biomass feedstock (Wang et al. 2013a, 2013b; Lei et al. 2014; Li et al. 2019; Dong et al. 2022a) are the raw materials for LaA synthesis. The conversion of cellulose to LaA is more

difficult than that of monosaccharides because it needs the selective activation and breaking of certain C–O and C–C bonds (Li et al. 2019) (Scheme 1). Catalysts for cellulose to LaA conversion include homogeneous and heterogeneous catalysts. Homogeneous catalysts often use metal salt catalysts (Al^{3+} , VO^{2+} , Pb^{2+} , Zn^{2+} and Sn^{2+}) (Zhang et al. 2011; Wang et al. 2013a, 2013b; Tang et al. 2014; Deng et al. 2018a, 2018b) and alkaline catalysts (NaOH , $\text{Ca}(\text{OH})_2$, $\text{Ba}(\text{OH})_2$) (Esposito and Antonietti 2013). However, due to the difficulties of separation and recovery, the strong corrosiveness of alkaline conditions, and the occurrence of side reactions with sugar compounds, their large-scale application is limited (Gezae Daful and Görgens 2017).

In comparison, heterogeneous catalysts are more attractive for industrial use. Currently, metal oxides, molecular sieves, metal-organic frameworks, aluminum-silicate oxide-supported metals and carbon-based solid acid catalysts have been used in the conversion of glyceraldehyde, glucose, and cellulose to LaA (Rahaman et al. 2022; Kupila et al. 2021; Huang et al. 2017; Shen et al. 2019; Xiao et al. 2022; Xu et al. 2022). The yield of LaA was 24% using LaCoO_3 perovskite metal as a catalyst for cellulose conversion (Yang et al. 2016). $\text{Sn-KIT-6-Pr-SO}_3\text{H}$ was employed for cellulose conversion, yielding 16.2% LaA and 88.9% cellulose conversion (Cai et al. 2019). Efficient conversion of cellulose to LaA on yttrium-modified beta zeolite, achieving LaA yields of up to 49.2% (Ye et al. 2021). $\text{TSA/SiO}_2\text{-Al}_2\text{O}_3$ was used as the catalyst to achieve LaA yield of 23.5%, selectivity of 38.4% and cellulose conversion of 61.2% (Marianou et al. 2019). In addition, a maximum LaA production of 42% was attained by using lignin-based activated carbon-supported metal oxides as catalysts to create LaA from glucose (Kupila et al. 2021). Many studies have shown that preparing supported catalysts is an effective way to reduce catalyst costs and improve catalytic performance (Yang et al. 2020). Compared with molecular sieves and metal-organic frameworks, lignin-based carbon materials are cheaper, simpler to prepare, and have more environmentally friendly chemical production processes. They can also be used as co-catalysts to improve catalytic activity, enhancing their chemical and physical properties by modifying their specific surface functional groups and pore structures (Pérez-Mayoral et al. 2016; Zhang et al. 2022).



Scheme 1 Reaction route of cellulose into LaA and main byproducts

In this work, lignin-based carbonaceous support (LCSA) was prepared by one-step sulphonation and carbonization with chlorosulfonic acid and lignin-based solid acid catalysts were obtained by loading amphoteric metals Al and Zn on the support. The prepared catalysts were used to test the catalytic activity in the conversion of *Pueraria* cellulose to LaA. It was found that LCSA–Al could effectively convert *Pueraria* cellulose to LaA in an aqueous solution, and the substrate could be extended to biomass from other sources.

Materials and methods

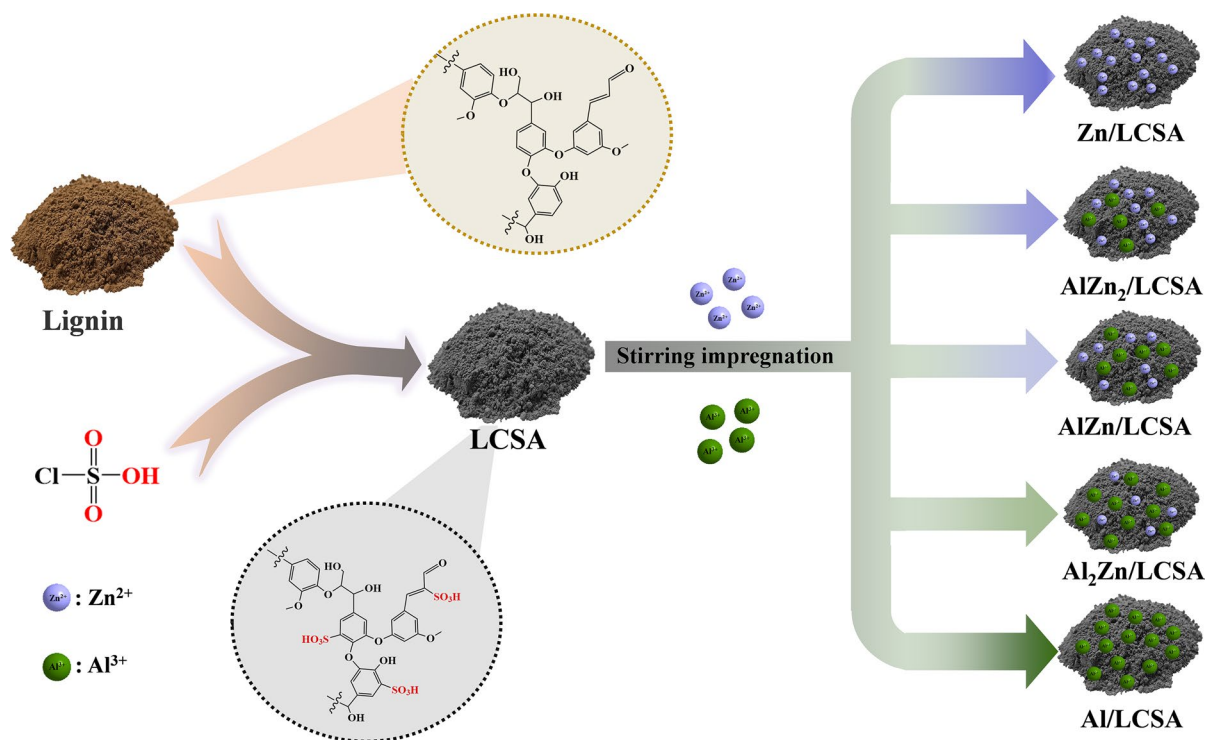
Materials

P. edulis Pampan. residue was obtained from Hunan Zhangjiajie Jiutian Biotechnology Co., Ltd; Lignin was bought from the Shandong Longlive Bio-technology Co., Ltd; dichloromethane ($\geq 99.5\%$) was purchased from Shanghai Titan Scientific Co., Ltd, Shanghai, China; Chloro-sulfonic acid (99.0%) was purchased from Energy Chemical Co., Ltd, Shanghai,

China; $\text{AlCl}_3 \cdot 6\text{H}_2\text{O}$ (AR) and ZnCl_2 (AR) and 5-Hydroxymethylfurfural (HMF, 97%) were bought from Sinopharm Chemical Reagent Co., Ltd. LaA (99%) was purchased from Shanghai Nature Standard Technical Services Co., Ltd. All chemicals were used as supplied without any further purification. Deionized water used in this work was prepared using a water purification system (Heal Force, Shanghai Shengke Equipment Co., Ltd., Shanghai, China).

Extraction of *Pueraria* cellulose

Similar to our previous investigation, the *Pueraria* cellulose extraction technique was carried out (Peng et al. 2022). The specific extraction method is as follows: the washed *P. edulis* Pampan. residue was crushed and 5 g were placed in 250 mL of sodium chlorite solution with a concentration of 4%. The pH value was adjusted to 3–4 with concentrated hydrochloric acid, and the residue was treated at 100 °C for 2 h. The obtained residue was washed with deionized water until the aqueous solution was neutral. Dry at 100 °C to obtain *P. edulis* Pampan. residue after sodium chlorite treatment. The 5 g of the



Scheme 2 Preparation of lignin-derived carbon-based solid acid catalysts

powder treated with sodium chlorite was put in 250 mL sodium hydroxide solution with 15% concentration and treated at 80 °C for 2 h. The residue was washed with deionized water until the aqueous solution was neutral. After drying at 100 °C, *Pueraria* cellulose with 94% purity was obtained.

Preparation of catalysts

Preparation of LCSA

The carbonaceous support was prepared from lignin by one-step carbonization and sulfonation with chlorosulfonic acid. The composition of used lignin is provided in Table S1 (Supplementary material). In an ice-water bath, 2 g of lignin was added to a round-bottom flask containing 30 mL of dichloromethane and stirred. Then 4.5 mL (15% dichloromethane) chlorosulfonic acid was added drop by drop to the mixed solution. The mixture was stirred in a nitrogen atmosphere for 6 h, and then anhydrous ethanol was cautiously added to the round-bottom flask until no bubbles were generated in the flask. Finally,

centrifuged to remove dichloromethane and anhydrous ethanol. Eventually, the remaining solids were dried in a vacuum oven at 60 °C for 12 h. The support was named LCSA.

Preparation of the catalyst

The LCSA- Al_xZn_y catalyst was prepared by the impregnation method. The specific operation is shown in Scheme 2. In a typical preparation method, 0.01 mol $\text{AlCl}_3 \cdot 6\text{H}_2\text{O}$ and 0.01 mol ZnCl_2 were prepared as 0.2 mol/L solutions, respectively. LCSA and the solution configured above were mixed in a mass ratio of Al_xZn_y :LCSA = 1:2 (x and y respectively represent the proportion of Al and Zn in the load solution calculated according to mass) and stirred for 24 h until evenly dispersed. Suction filtration and washing until the filtrate was close to neutral. The obtained suspension was dried in an oven at 105 °C for 12 h to remove water. The prepared catalysts are named LCSA-Al, LCSA-Zn, LCSA-AlZn, LCSA-Al₂Zn, LCSA-AlZn₂.

Catalyst characterization

The catalyst samples, *Pueraria* cellulose and *P. edulis* Pampan. residues were characterized and analyzed on a scanning electron microscope (SEM, QUANTA FEG 450). The morphology of samples was observed at 15 kV. Energy-dispersive spectroscopy (EDS) was performed using an X-Max instrument (Oxford Instruments). The prepared catalyst powder was characterized using a SmartLab9 X-ray diffractometer from RIKEN, Japan. The radiation source was Cu-K α ($\lambda=0.15416$ nm), and the device was used to record X-ray diffractograms at a sample voltage and current of 40 kV and 40 mA, respectively, and a scan rate of $10^\circ \text{ min}^{-1}$. The diffractograms were collected at 0.02° intervals in the 2θ range of 5° – 90° . The specific surface area of the catalysts was determined on a TriStar II Plus 3030 physisorption instrument shipped from Mack, USA. Nitrogen adsorption–desorption measurements were performed at -196° C to obtain the specific surface area of the catalysts, and the average pore size and pore volume of the samples were calculated using the BJH method. Before measurement, the samples were heated in a vacuum at 140° C for 3 h to eliminate moisture and volatile contaminants.

Infrared analysis of the catalysts was performed using a Fourier transform infrared (FT-IR) spectrometer (Nicolet-iS10, Thermo Scientific, USA) with a wave number range of 400 – 4000 cm^{-1} . To determine the total acidity of the catalyst, NH_3 -TPD (programmed ramp-up desorption) was performed in a BELCAT (Bayer, Japan) analyzer. The sample tubes were filled with 0.1 g of catalyst and pretreated at 350° C for 30 min in a helium atmosphere. After cooling to 100° C , the sample was placed in an NH_3/He (5%) gas stream for 1 h. The physically adsorbed NH_3 was then removed using a dry helium stream for 30 min. Finally, TPD was measured in the dry helium stream at a heating rate of $10^\circ \text{ C min}^{-1}$ from 100 to 800° C .

Catalyst performance tests

All reactions were performed in a 25 mL batch-type Teflon-lined stainless-steel autoclave. In a typical catalytic experiment, 50 mg of *Pueraria* cellulose, 50 mg of catalyst, and 10 mL of water were charged into the reactor. The reaction mixture was heated to the necessary reaction temperature for a time with

stirring at 600 rpm. Then the test reactor was taken out of the oil bath, then cooled quickly to room temperature with plenty of cold water. The liquid mixture was passed through a $0.45\text{-}\mu\text{m}$ filter and analyzed by high-performance liquid chromatography (HPLC) after the reaction.

The LaA yield was determined using an HPLC (Agilent-1260, USA) equipped with an ultraviolet-visible detector ($\lambda=210$ nm). A C18 reversed-phase chromatographic column (Waters, 250×4.6 mm, $5 \mu\text{m}$) was used for chromatographic separation. A mobile phase of 0.1% phosphoric acid water and acetonitrile (95:5, v/v) was used for the isocratic elution. The column temperature was 30° C . The flow rate and injection volume were maintained at 0.5 mL/min , and $20 \mu\text{L}$, respectively. The conversion of *Pueraria* cellulose and the yields of the products (weight based) were calculated according to the follows:

$$\text{Conversion}_{\text{cellulose}}(\%) = 100 \times \frac{\text{Pueraria cellulose reacted (g)}}{\text{Pueraria cellulose initial (g)}} \quad (1)$$

$$\text{Yield}_{\text{product}}(\%) = 100 \times \frac{\text{product produced (g)}}{\text{Pueraria cellulose initial (g)}} \quad (2)$$

Results and discussion

P. edulis Pampan. Residue and *Pueraria* cellulose characterization

Figure 1 demonstrates the SEM results of *P. edulis* Pampan. residue and *Pueraria* cellulose. The surface of the *P. edulis* Pampan. residue was rough and stuck to one another, as can be seen in Fig. 1a. The diameter of *P. edulis* Pampan. residue is about $120 \mu\text{m}$. After the two-step treatment with NaClO_2 and NaOH , Fig. 1b shows that the *Pueraria* cellulose disintegrated into rods, and its diameter is about $18 \mu\text{m}$, indicating that the non-cellulose components of the *P. edulis* Pampan. residue was successfully eliminated and high purity of *Pueraria* cellulose was produced.

There are various crystal forms of cellulose, and each crystal form has unique physicochemical features. As seen in Fig. S1, the diffraction peaks for *P. edulis* Pampan. residue and *Pueraria* cellulose appear at $2\theta=15.2^\circ$, 16.4° , 22.8° , and 34.9° , respectively. These peaks correspond to the cellulose

Fig. 1 SEM images of (a) *P. edulis* Pampan. residue and (b) *Pueraria* cellulose

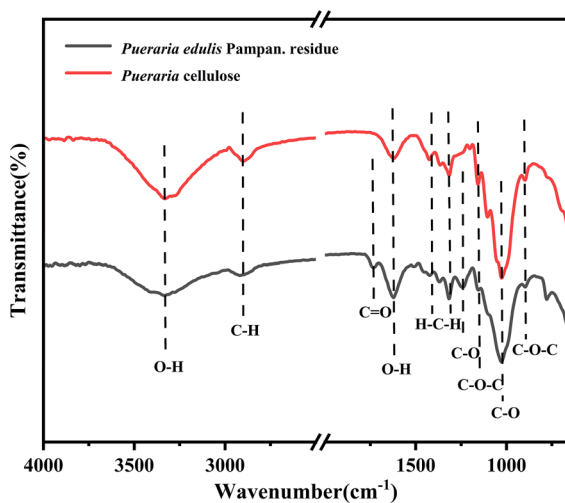
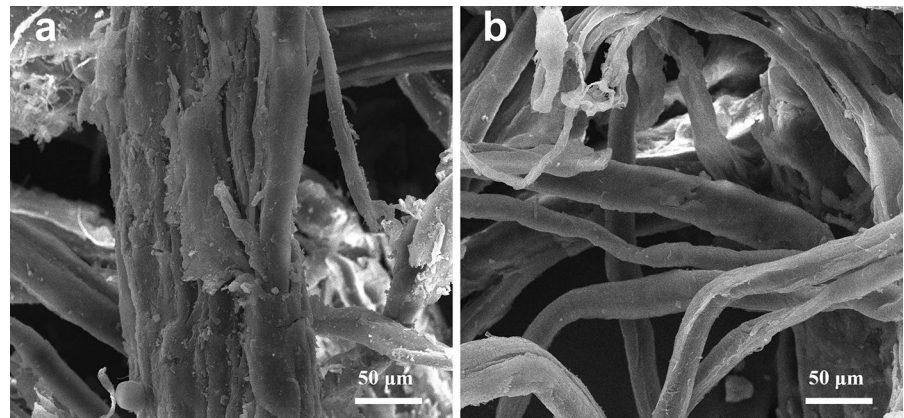


Fig. 2 FT-IR analysis of *P. edulis* Pampan. residue and *Pueraria* cellulose

(1₁₀), (110), (200), and (004) crystal planes, indicating that they belong to cellulose I (Tarchoun et al. 2019). The continuity of the diffraction peaks did not change after the chemical treatment implying that the chemical treatment had no impact at all on the cellulose crystal structure. According to the crystallinity index equation (Kian et al. 2017), the crystallinity of *P. edulis* Pampan. residue and *Pueraria* cellulose were 54.4% and 71.5%, respectively. The removal of the non-cellulose components from the *P. edulis* Pampan. residue may also be suggested by an increase in crystallinity.

FT-IR was used to determine the chemical compositions and functional groups of samples. According to Fig. 2, the O–H stretching vibration and the C–H

asymmetric stretching vibration of the cellulose glucose unit, respectively, caused noticeable peaks in all samples at about 3333 and 2917 cm^{-1} (Fareez et al. 2018). In this wave number range, the peak shoulders of *Pueraria* cellulose widened. This is caused by the exposure of cellulose and the removal of non-cellulose *P. edulis* Pampan. residue components. All of the samples had a characteristic peak at 1622 cm^{-1} , which was generated by the O–H bending vibration of the water absorption peak adsorbed on the sample surface. Other characteristic peaks included those at 1423 and 1316 cm^{-1} , which were caused by the H–C–H bending and stretching vibrations of the cellulose glucose unit. 1157 cm^{-1} , which was caused by the C–O–C asymmetric vibrations on the cellulose glucose ring. 1027 cm^{-1} by C–O stretching vibration, and the characteristic peak around 898 cm^{-1} was caused by C–O–C stretching vibration of β -1,4 glycosidic bond (Sun et al. 2005; Yue et al. 2019; Tanpichai et al. 2019). The difference is that the absorption peaks around 1730 and 1245 cm^{-1} of *P. edulis* Pampan. residue corresponds to C=O connecting hemicellulose to the acetyl or glyoxylate group of lignin (Sain and Panthapulakkal 2006) and C–O of lignin (Tarchoun et al. 2019), respectively, while the absorption peak of *Pueraria* cellulose disappears here. It indicates that the lignin and hemicellulose of *P. edulis* Pampan. residue was effectively removed after two steps of NaClO_2 and NaOH treatment.

Catalyst characterization

As shown in Fig. 3, the image adopts SEM mode, and at the same time, combines EDS analysis and quantitative mapping to detect the elemental composition

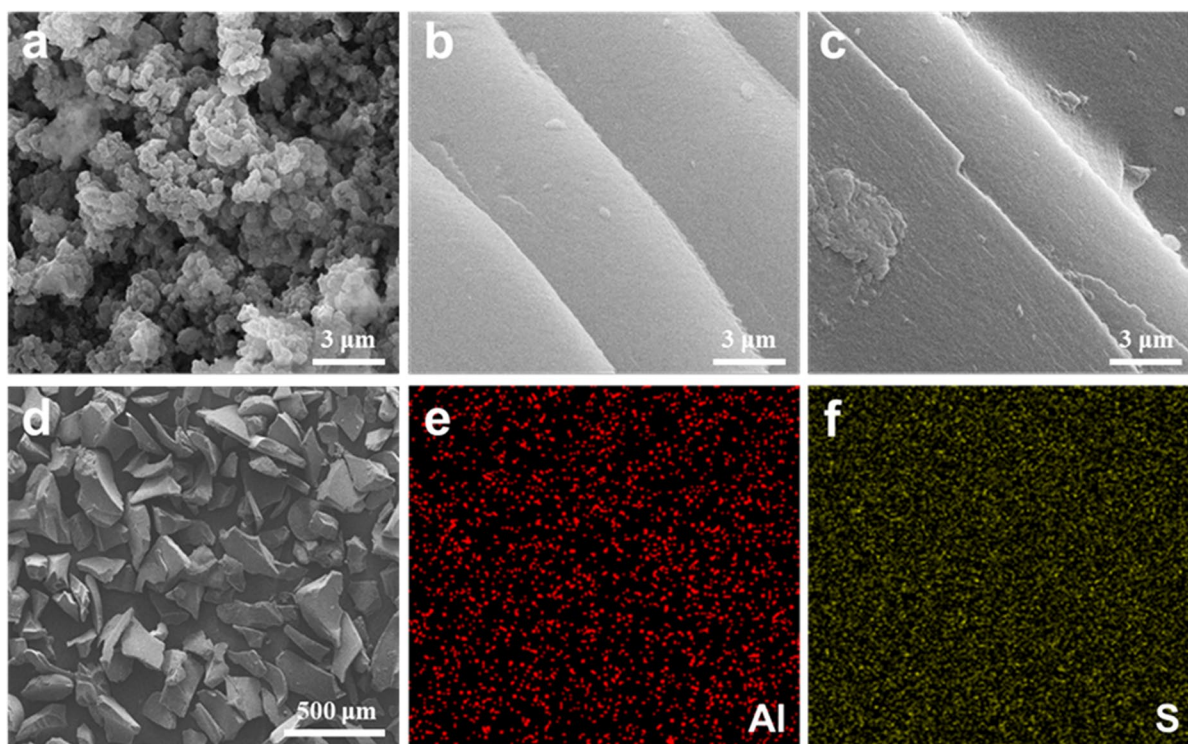


Fig. 3 SEM images of (a) LI–3 μm , (b) LCSA–3 μm , (c) LCSA–Al–3 μm and (d) LCSA–500 μm . SEM-EDS elemental mappings of LCSA–Al, with the coloring of the (e) aluminum (red) and (f) sulfur (green)

of the material. SEM image of LI (a) displayed an irregular shape formed by a large number of spherical particles. Lignin after one-step sulfonation carbonization LCSA (d) shows heterogeneous polyhedral morphology (Balasubramanian and Venkatachalam, 2022). A large number of cracks on the outer surface of the carbon carrier, and this morphological feature facilitates the formation of outstanding catalytic properties and a stabilized carbon skeleton structure. This stable carbon skeleton structure can provide an effective reaction site, which can ensure the effective binding of sulfonic acid groups to the inner and outer surfaces of the carbon carrier, resulting in an increase in the total acidity of the catalyst and also promoting the subsequent hydrolysis reaction. More cellulose molecules enter the catalyst to undergo hydrolysis, isomerization, and other chemical reactions with hydrogen ions, thereby increasing the yield of LaA. The uniform distribution of aluminum and zinc on the surface of LCSA was observed in the SEM-EDS elemental mappings image of LCSA–Al (Fig. 3), LCSA–Zn (Fig.S2), LCSA–AlZn, LCSA–Al₂Zn and

LCSA–AlZn₂, respectively, indicating the successful loading of Al and Zn onto the lignin carbon-based carrier. The homogeneous distribution of sulfur elements indicates the successful grafting of sulfonate onto the carrier.

XRD patterns of lignin (LI), after sulfonation carbonization (LCSA) and loading metal Al after sulfonation and carbonization (LCSA–Al) are presented in Fig. S3. As depicted in Fig. S3, there is no strong peak in the whole XRD spectrum, indicating that the material does not exist crystal structure. A broad peak at 2θ 20–25° and a weak characteristic peak at 40–50° signifies the C (002) and C (101) plane of graphite crystallites, respectively. These peaks accord with randomly permutation amorphous carbon with low crystalline graphite content (Balasubramanian and Venkatachalam, 2022). Therefore, lignin-based solid acid is a polycyclic aromatic compound with an amorphous carbon structure (Gan et al. 2017). Studies have shown that the amorphous carbon structure is conducive to the loading of SO₃H groups to prepare solid acid

catalysts (Wang et al. 2022). Compared with the diffraction pattern of lignin, the diffraction peak of sulfonated carbon shifted slightly to the right, which may be due to the strong oxidation characteristics of chlorosulfonic acid and carbon (Gan et al. 2017).

No clear peak was detected for Al, possibly due to small particle size or low concentration of the catalyst material. Overall, the diffraction pattern shows that the crystallinity of Al is not high, indicating the presence of an amorphous phase or very small particles on the surface of the support (Kupila et al. 2021), which can also be seen in the SEM-EDS elemental mappings image.

It can be seen from the nitrogen adsorption-desorption isotherm (Fig. 4) that the material exhibits typical characteristics of mesoporous material with type IV isotherm and H3 hysteresis loop (Tong et al. 2022). As shown in Table 1, Compared with lignin, the specific surface area, pore volume and pore diameter of the lignin carbon-based catalyst are all reduced, which is due to the metal is loaded on the surface of the lignin carbon-based support or enters its pore channels. The pore diameter of LCSA is larger than LCSA–Zn, LCSA–AlZn, LCSA–AlZn₂ and LCSA–Al₂Zn. The high catalytic activity of LCSA–Al may be attributed to its wide pore diameter, which enables the *Pueraria* cellulose to make more complete contact with the catalyst's active site.

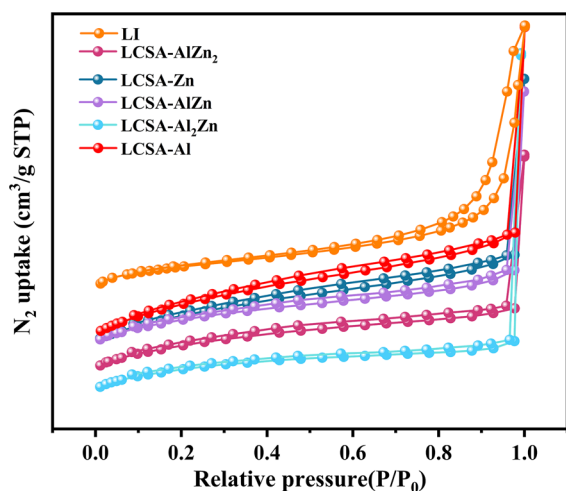


Fig. 4 N₂ adsorption–desorption isotherms of the LI and LCSA, LCSA–Al, LCSA–Zn, LCSA–AlZn, LCSA–AlZn₂ and LCSA–Al₂Zn

Table 1 Specific surface areas and pore sizes and pore volume of LI and catalysts

Sample	BET surface area (m ² g ⁻¹)	Average pore diameter (nm)	Total pore volume (cm ³ g ⁻¹)
LI	32.23	16.64	0.124
LCSA–Al	2.03	9.37	0.022
LCSA–Zn	2.72	4.24	0.017
LCSA–AlZn	3.35	4.57	0.014
LCSA–Al ₂ Zn	2.66	4.66	0.010
LCSA–AlZn ₂	2.18	4.39	0.012

The LI, LCSA and LCSA–Al chemical structures were characterized with FT-IR analysis (Fig. 5). All spectra show a wide transmittance band at 3200–3600 cm⁻¹ with a maximum at roughly 3417–3430 cm⁻¹. This band can be assigned to the O–H stretching mode of hydroxyl groups and adsorbed water (Kusuma et al. 2021). The C–H absorption peaks near 3000 cm⁻¹ and 869 cm⁻¹ are located in the aromatic skeleton, respectively (Li et al. 2018). It can be seen from the figure that after loading the metal Al, the C–H absorption peak of LCSA–Al is weakened, possibly because Al replaces H on the C–H bond. The peak at 1700 cm⁻¹ was attributed to the C=O stretching vibration (Sangsiri et al. 2022); the stretching vibration peaks of S=O and C–S were at 1030 cm⁻¹ and 645 cm⁻¹, respectively. This means that –SO₃H

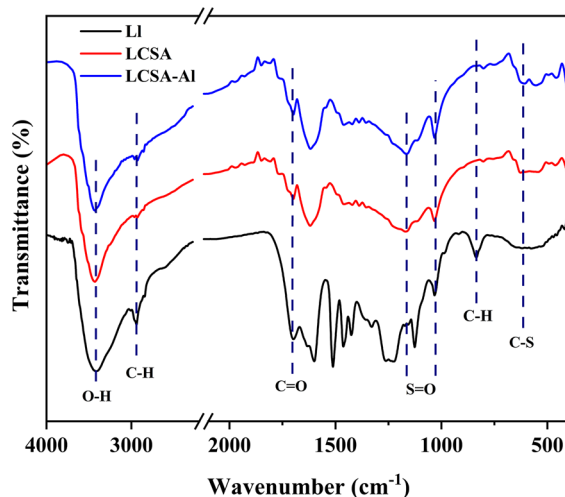


Fig. 5 FT-IR analysis of LI, LCSA and LCSA–Al catalysts

is successfully attached to the surface of the lignin-based carbon skeleton by replacing H on the carbon material skeleton and by forming covalent bonds with the skeleton (Suganuma et al. 2011).

NH_3 -TPD analyses were used to detect the acid strength of catalyst surfaces. Desorption peak temperatures above 350 °C are considered to belong to strong acidic sites, 200–350 °C is medium-strong acidic sites, and below 200 °C is weak acidic sites (Xu et al. 2022). From the Fig. 6, it can be seen that LCSA exhibits a small desorption peak centered around 175 °C, followed by a relatively strong and broad NH_3 desorption peak in the range of 450–600 °C, indicating that the surface of this sample has two different types of acidic sites: weak and strong. The sample has strong acidity because a large number of sulfonic acid groups were grafted on the carbonaceous support after the treatment of lignin with chlorosulfonic acid. The FT-IR (Fig. 5) characterization also proved that the sulfonic acid group was successfully grafted on the carbonaceous support. As can be seen from Table 2, when metal ions were loaded on the lignin-based carbon support, the surface acidity was significantly increased, and the surface acidity of LCSA–Al (1.54 mmol/g), LCSA–AlZn (2.32 mmol/g), LCSA–Al₂Zn (1.97 mmol/g) and LCSA–AlZn₂ (1.49 mmol/g) were significantly enhanced compared to LCSA (0.64 mmol/g). Additionally, compared to LCSA–Al (1.54 mmol/g), LCSA–AlZn (2.32 mmol/g) and LCSA–Al₂Zn (1.97

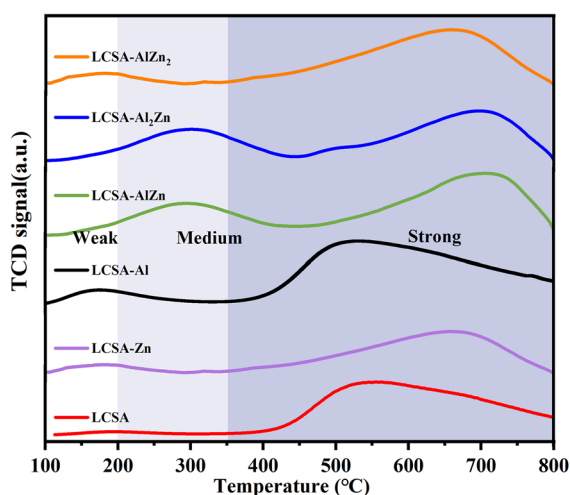


Fig. 6 NH_3 -TPD profiles of LCSA, LCSA–Al, LCSA–Zn, LCSA–AlZn, LCSA–AlZn₂ and LCSA–Al₂Zn

Table 2 Total amount of acidity of catalysts determined by NH_3 -TPD.

Sample	Total amount of acidity (mmol/g)
LCSA	0.64
LCSA–Al	1.54
LCSA–Zn	1.06
LCSA–AlZn	2.32
LCSA–Al ₂ Zn ₁	1.97
LCSA–AlZn ₂	1.49

mmol/g) had higher acid densities. It is concluded that the excellent catalytic performance of LCSA–Al may be due to its appropriate acid site density.

Screening of catalysts

The catalytic performances of no catalyst, LCSA, and different Al/Zn ratios loaded on LCSA were investigated. The conversion rate of *Pueraria* cellulose and the yield of LaA are shown in Table 3. The blank experiment obtained a LaA yield of 2.4%, which was much lower than the LaA yield obtained with the participation of catalysts, indicating that the series of prepared lignin-based carbon solid acid catalysts have high activity. The catalytic performance of LCSA was relatively weak among all the prepared lignin-based carbon solid acid catalysts, indicating that Brønsted acid alone is not sufficient for cellulose conversion to LaA. The principal by-product of the process of converting *Pueraria* cellulose into LaA is HMF, along with a trace of formic acid, acetic acid,

Table 3 Screening of catalysts

Entry	Catalyst	Yield (%)		Conversion (%)
		LaA	HMF	
1	Blank	2.4	0.7	8.4
2	LCSA	7.4	2.7	49.2
3	LCSA–Zn	12.5	2.5	76.3
4	LCSA–Al	21.5	3.1	64.7
5	LCSA–AlZn	14.6	2.4	71.8
6	LCSA–AlZn ₂	13.4	2.4	73.9
7	LCSA–Al ₂ Zn	15.7	2.9	68.5

Reaction conditions: *Pueraria* cellulose, 50 mg; catalyst, 50 mg; water, 10 mL; 180 °C, 2 h

and levulinic acid (Lei et al. 2014). With the increase of the aluminum content in the catalyst, the yield of LaA increases, indicating that aluminum is more conducive to promoting the conversion of *Pueraria* cellulose to LaA than zinc. From the data in the Table 3, surprisingly, when the content of Zn in the catalyst increases, the conversion rate of *Pueraria* cellulose increases while the yield of LaA decreases. Suggesting that zinc can promote *Pueraria* cellulose to convert to other pathways. Based on the preliminary research results, LCSA–Al was determined as the catalyst with the best effect according to the yield of LaA. LCSA–Al was further analyzed for the production of LaA.

Effect of reaction time and reaction temperature on catalytic reaction

Using LCSA–Al as the catalyst based on the preliminary screening of the catalysts, the effects of reaction time (0.5–3.0 h) and temperature (140–200 °C) on the conversion rate of *Pueraria* cellulose (Fig. 7b) and LaA yield (Fig. 7a) were investigated. It can be observed that when the temperature rises, the rate of cellulose conversion also improves, indicating that high temperature is conducive to cellulose hydrolysis. At 200 °C, the conversion rate increased dramatically within 1 h and reached 100% in 3 h. At lower temperatures (140–160 °C), cellulose can also

be hydrolyzed, and it was speculated that the strong Brønsted acidity exhibited by $-\text{SO}_3\text{H}$ in LCSA–Al promotes the cleavage of cellulose glycosidic bonds and its hydrolysis (Li et al. 2018). In Fig. 7a, it was found that before 1 h of reaction, the LaA yield raises as the reaction temperature goes up (140–180 °C), especially at 160 °C where the yield increase is most significant. After 1 h of reaction, the LaA yield at 180 °C shows a decreasing trend with increasing reaction time due to the production of by-products (such as humic acid and HMF). The LaA yield at 200 °C was very low, suggesting that side reactions occur under this temperature. At 160 °C, although the conversion rate of *Pueraria* cellulose was not as high as that at 180 °C and 200 °C, the LaA yield grows initially before declining over time, reaching the maximum value (24.7%) at 2 h. Therefore, 160 °C and 2 h were chosen as the optimal reaction temperature and time.

Effect of catalyst dosage on catalytic performance

After determining the optimal reaction time and temperature, the effect of catalyst dosage on the hydrolysis products of *Pueraria* cellulose was investigated, as shown in Fig. 8. It can be observed that with increasing catalyst dosage, the LaA yield first increases and then decreases. When the catalyst dosage was less than 0.05 g, some soluble oligosaccharides in the

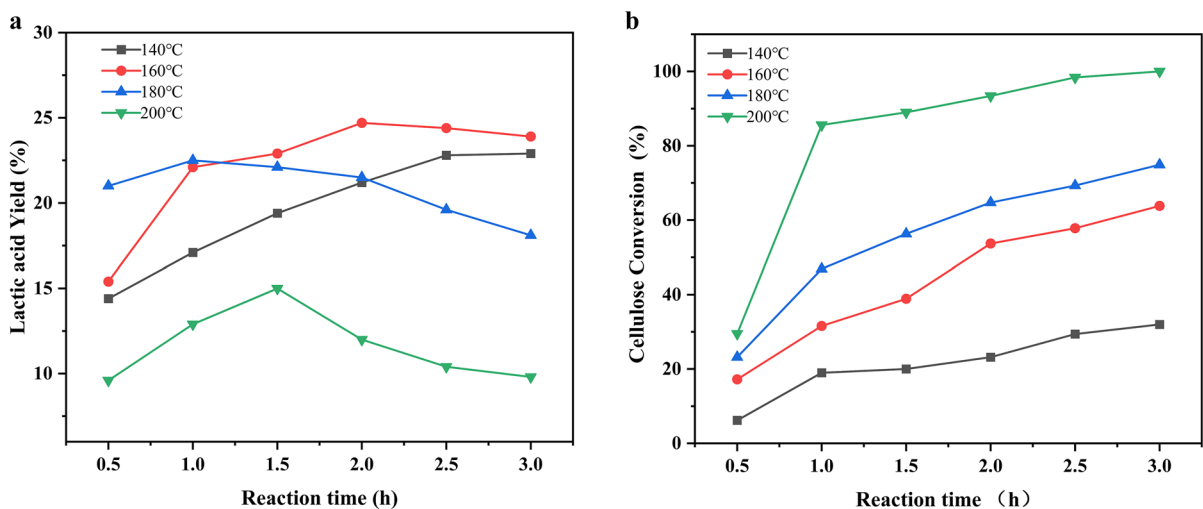


Fig. 7 Effects of reaction time and temperature on the yield of LaA (a) and the conversion rate of *Pueraria* cellulose (b) were studied. Reaction conditions: *Pueraria* cellulose, 50 mg; catalyst, 50 mg; water, 10 mL; 600 rpm

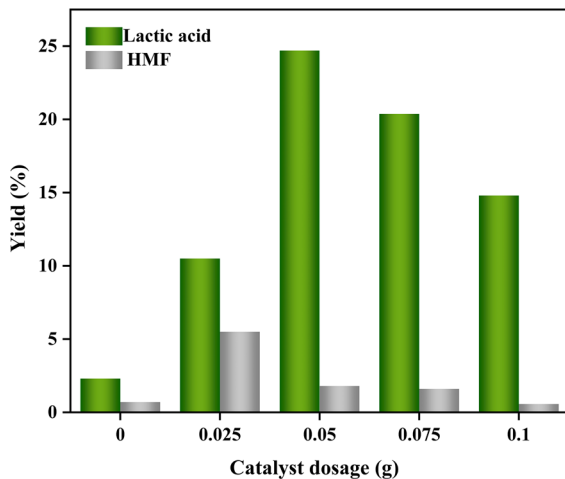


Fig. 8 Effect of catalyst dosage on the yield of LaA from *Pueraria* cellulose. Reaction conditions: *Pueraria* cellulose, 50 mg; water, 10 mL; 160 °C; 2 h, 600 rpm

reaction system were not completely converted during the cellulose depolymerization process, leading to a lower LaA yield. When the catalyst dosage was 0.05 g, the LaA yield reaches the highest value of 24.7%. A higher concentration of active sites may aid to promote additional polymerization of LaA and form soluble polymers, humus, and unwanted by-products, which causes a drop in LaA yield when the catalyst dosage is increased further (Dong et al. 2022a). Table 4 provides a summary of some of the heterogeneous catalysts used to convert cellulose into LaA. Despite having higher LaA outputs than other metals, rare earth metals are pricey and unsuitable for industrial use. In comparison to these results, our catalyst

delivered acceptable LaA yields during cellulose conversion at lower temperatures and in less time.

Effect of reaction solvent on catalytic reaction

In exploring the effect of reaction solvent on LaA selectivity (Fig. 9), it was found that using wholesome and non-toxic water as the reaction solvent resulted in the highest yield. This is because using water as the reaction solvent allows more cellulose molecules to enter the catalyst to undergo hydrolysis with hydrogen ions, isomerization and other chemical reactions to increase the yield of LaA.

Applied to the conversion of other carbohydrates

The catalyst was applied to the conversion of other carbohydrates (Fig. 10) and it was found that the conversion of fructose to LaA resulted in a higher yield than that of glucose to LaA. This is due to the fact that aldose glucose is first isomerized during the process to create ketose fructose (Kupila et al. 2021), which requires the consumption of some heat. Sucrose is formed by the condensation of one molecule of glucose and one molecule of fructose, and the yield of LaA prepared from sucrose as a raw material is between the two. The yield of starch to LaA (29%) was found to be higher than the yield of *Pueraria* cellulose to LaA. This is due to the β -1,4 glycosidic linkage connecting the glucose monomer in cellulose, which are more challenging to hydrolyze than the α -1,4 glycosidic linkage in starch. Xylose (C5 sugar) has a simpler structure than *Pueraria* cellulose and

Table 4 Summary of heterogeneous catalysts for the conversion of biomass to LaA

Catalyst	Substrate	Conditions in conversion	Yield of LaA (%)	References
Sn-KIT-6-Pr-SO ₃ H	Cellulose (0.3 g)	Cat. (0.1 g); H ₂ O (30 g); 210 °C; 1 h; 5 Mpa N ₂	16.2	(Cai et al. 2019)
10% Y-Beta	Cellulose (0.3 g)	Cat. (0.1 g); H ₂ O (30 mL); 220 °C; 30 min; 2 Mpa N ₂	49.2	(Ye et al. 2021)
LaCoO ₃	Cellulose (1 mmol)	Cat. (4 mmol); H ₂ O (20 g); 240 °C; 1 h; 400 psi N ₂	24	(Yang et al. 2016)
TSA/SiO ₂ -Al ₂ O ₃	Cellulose (6 wt%)	Cat. (cellulose:cat = 1:1); H ₂ O; 24 h; 175 °C;	23.5	(Marianou et al. 2019)
LCSA-Al	<i>Pueraria</i> cellulose (50 mg)	Cat. (50 mg); H ₂ O (10 mL); 2 h; 160 °C;	24.7	This study

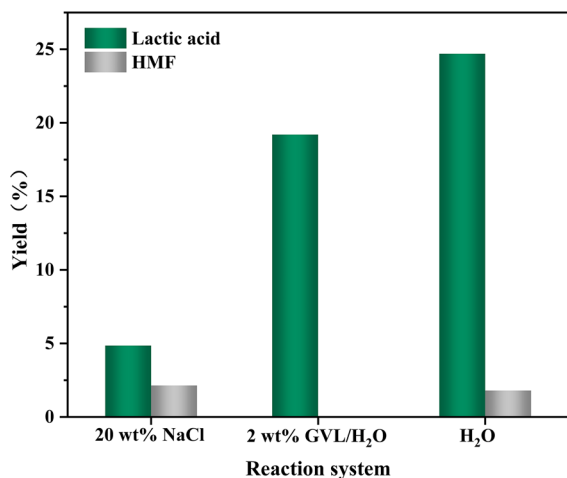


Fig. 9 Effect of reaction solvent on the conversion of *Pueraria* cellulose to LaA. Reaction conditions: *Pueraria* cellulose, 50 mg; catalyst, 50 mg; 160 °C; 2 h, 600 rpm

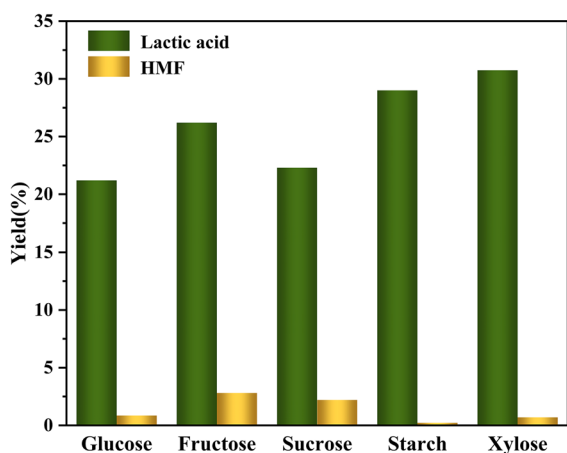


Fig. 10 Applied to the conversion of other carbohydrates to LaA. Reaction conditions: carbohydrates, 50 mg; catalyst, 50 mg; water, 10 mL; 160 °C; 2 h, 600 rpm

can be converted to LaA more easily. LaA was generated by xylose at a rate of 30.74%.

Conclusions

In this study, lignin-based carbonaceous carriers (LCSA) were prepared by a one-step sulfonation-carbonization method using chlorosulfonic acid. The effect of aluminum or zinc-containing catalysts

supported on the prepared LCSA on the conversion of *Pueraria* cellulose to LaA was investigated. The results showed that the prepared lignin carbon-based solid acids could effectively catalyze the conversion of *Pueraria* cellulose to LaA. The addition of aluminum was more favorable than zinc for obtaining a higher yield of LaA. LCSA–Al exhibited the best catalytic performance. LCSA–Al had Lewis acid and Brønsted acid sites, with fewer weak acid sites and more strong acid sites. At 160 °C, with 50 mg of *Pueraria* cellulose, 50 mg of catalyst and 10 mL of deionized water, the conversion rate of *Pueraria* cellulose was 53.7% and the yield of LaA was 24.7%. In addition to providing a chemical pathway for the transformation of related carbohydrates, this work develops a new approach for the future conversion of cellulose to LaA.

Acknowledgments Not applicable.

Author contributions HK is the first author of this study. KS is the corresponding author of this study, and he is supervisor of this project. HK and KS contributed to the study conception and design. JG and XG prepared Figures. Material preparation, data collection and analysis were performed by HK, KS, JH and XZ. The first draft of the manuscript was written by HK and all authors commented on previous versions of the manuscript. All authors read and approved the final manuscript.

Funding This work was supported by National Natural Science Foundation of China (No. 22268019), and the Natural Science Innovation Project of Jishou University (JGY2023061).

Data availability The data that support the findings of this study are available from the corresponding author upon request.

Declarations

Conflict of interest The authors declare no competing interests.

Consent for publication Written informed consent for publication was obtained from all participants.

References

- Balasubramanian S, Venkatachalam P (2022) Green synthesis of carbon solid acid catalysts using methane sulfonic acid and its application in the conversion of cellulose to platform chemicals. *Cellulose* 29(3):1509–1526. <https://doi.org/10.1007/s10570-022-04419-7>
- Cai W, Chen Q, Xuan H, Li C, Yu H, Cui L, Yu Z, Zhang S, Qu F (2019) One-pot synthesis of lactic acid from

- cellulose over a sulfonated Sn-KIT6 catalyst. *Korean J Chem Eng* 36(4):513–521. <https://doi.org/10.1007/s11814-019-0236-8>
- Castillo Martínez FA, Balciunas EM, Salgado JM, Domínguez González JM, Converti A, Oliveira RPDS (2013) Lactic acid properties, applications and production: a review. *Trends Food Sci Technol* 30(1):70–83. <https://doi.org/10.1016/j.tifs.2012.11.007>
- Chen SS, Tsang DCW, Tessonnier J (2020) Comparative investigation of homogeneous and heterogeneous Brønsted base catalysts for the isomerization of glucose to fructose in aqueous media. *Appl Catal B* 261:118126. <https://doi.org/10.1016/j.apcatb.2019.118126>
- Chen Z, Zhang S, Yan B, Cai Q, Zhang S (2022) Lignin-based solid acid catalyst for cellulose residue conversion into levulinic acid in biphasic system. *Ind Crops Prod* 178:114523. <https://doi.org/10.1016/j.indcrop.2022.114523>
- Dapsens PY, Mondelli C, Pérez-Ramírez J (2013) Highly selective lewis acid sites in desilicated MFI zeolites for dihydroxyacetone isomerization to lactic acid. *Chemsuschem* 6(5):831–839. <https://doi.org/10.1002/cssc.201200703>
- Deng W, Wang P, Wang B, Wang Y, Yan L, Li Y, Zhang Q, Cao Z, Wang Y (2018) Transformation of cellulose and related carbohydrates into lactic acid with bifunctional Al(iii)–Sn(ii) catalysts. *Green Chem* 20(3):735–744. <https://doi.org/10.1039/c7gc02975f>
- Deng W, Wang Y, Zhang S, Gupta KM, Hülsey MJ, Asakura H, Liu L, Han Y, Karp EM, Beckham GT, Dyson PJ, Jiang J, Tanaka T, Wang Y, Yan N (2018) Catalytic amino acid production from biomass-derived intermediates. *Proc Natl Acad Sci USA* 115(20):5093–5098. <https://doi.org/10.1073/pnas.1800272115>
- Dong W, Ou M, Qu D, Shi X, Guo M, Liu G, Wang S, Wang F, Chen Y (2022) Rare-earth metal yttrium-modified composite metal oxide catalysts for high selectivity synthesis of biomass-derived lactic acid from cellulose. *ChemCatChem* 14(12):e202200265. <https://doi.org/10.1002/cctc.202200265>
- Dusselier M, Van Wouwe P, Dewaele A, Makshina E, Sels BF (2013) Lactic acid as a platform chemical in the biobased economy: the role of chemocatalysis. *Energy Environ Sci* 6(5):1415–1442. <https://doi.org/10.1039/c3ee00069a>
- Esposito D, Antonietti M (2013) Chemical conversion of sugars to lactic acid by alkaline hydrothermal processes. *Chemsuschem* 6(6):989–992. <https://doi.org/10.1002/cssc.201300092>
- Fareez IM, Ibrahim NA, Wan Yaacob WMH, Mamat Razali NA, Jasni AH, Abdul Aziz F (2018) Characteristics of cellulose extracted from Jospine pineapple leaf fibre after alkali treatment followed by extensive bleaching. *Cellulose* 25(8):4407–4421. <https://doi.org/10.1007/s10570-018-1878-0>
- Feliczak-Guzik A, Sprynskyy M, Nowak I, Buszewski B (2018) Catalytic isomerization of dihydroxyacetone to lactic acid and alkyl lactates over hierarchical zeolites containing tin. *Catalysts* 8(1):31. <https://doi.org/10.3390/catal8010031>
- Gan L, Zhu J, Lv L (2017) Cellulose hydrolysis catalyzed by highly acidic lignin-derived carbonaceous catalyst synthesized via hydrothermal carbonization. *Cellulose* 24(12):5327–5339. <https://doi.org/10.1007/s10570-017-1515-3>
- Gezae Daful A, Görgens JF (2017) Techno-economic analysis and environmental impact assessment of lignocellulosic lactic acid production. *Chem Eng Sci* 162:53–65. <https://doi.org/10.1016/j.ces.2016.12.054>
- Guo L, Li J, Yuan Y, Gui Y, Zou F, Lu L, Cui B (2021) Structural and functional modification of kudzu starch using alpha-amylase and transglucosidase. *Int J Biol Macromol* 169:67–74. <https://doi.org/10.1016/j.ijbiomac.2020.12.099>
- Hossain MA, Mills KN, Molley AM, Rahaman MS, Tulaphol S, Lalvani SB, Dong J, Sunkara MK, Sathitsuksanoh N (2021) Catalytic isomerization of dihydroxyacetone to lactic acid by heat treated zeolites. *Appl Catal A Gen* 611:117979. <https://doi.org/10.1016/j.apcata.2020.117979>
- Huang S, Yang K, Liu X, Pan H, Zhang H, Yang S (2017) MIL-100(Fe)-catalyzed efficient conversion of hexoses to lactic acid. *Rsc Adv* 7(10):5621–5627. <https://doi.org/10.1039/c6ra26469g>
- Kian LK, Jawaid M, Ariffin H, Alothman OY (2017) Isolation and characterization of microcrystalline cellulose from roselle fibers. *Int J Biol Macromol* 103:931–940. <https://doi.org/10.1016/j.ijbiomac.2017.05.135>
- Kupila R, Lappalainen K, Hu T, Romar H, Lassi U (2021) Lignin-based activated carbon-supported metal oxide catalysts in lactic acid production from glucose. *Appl Catal A Gen* 612:118011. <https://doi.org/10.1016/j.apcata.2021.118011>
- Kusuma HD, Rochmadi, Prasetyo I, Ariyanto T (2021) Mesoporous manganese oxide/lignin-derived carbon for high performance of supercapacitor electrodes. *Molecules* 26(23):7104. <https://doi.org/10.3390/molecules26237104>
- Lei X, Wang F, Liu C, Yang R, Dong W (2014) One-pot catalytic conversion of carbohydrate biomass to lactic acid using an ErCl₃ catalyst. *Appl Catal A Gen* 482:78–83. <https://doi.org/10.1016/j.apcata.2014.05.029>
- Li Y, Shen S, Wang C, Peng X, Yuan S (2018) The effect of difference in chemical composition between cellulose and lignin on carbon based solid acids applied for cellulose hydrolysis. *Cellulose* 25(3):1851–1863. <https://doi.org/10.1007/s10570-018-1693-7>
- Li S, Deng W, Li Y, Zhang Q, Wang Y (2019) Catalytic conversion of cellulose-based biomass and glycerol to lactic acid. *J Energy Chem* 32:138–151. <https://doi.org/10.1016/j.jechem.2018.07.012>
- Lu Z, Demianets I, Hamze R, Terrile NJ, Williams TJ (2016) A prolific catalyst for selective conversion of neat glycerol to lactic acid. *ACS Catal* 6(3):2014–2017. <https://doi.org/10.1021/acscatal.5b02732>
- Marianou AA, Michailof CM, Pineda A, Iliopoulou EF, Triantafyllidis KS, Lappas AA (2016) Glucose to fructose isomerization in aqueous media over homogeneous and heterogeneous catalysts. *ChemCatChem* 8(6):1100–1110. <https://doi.org/10.1002/cctc.201501203>
- Marianou AA, Michailof CC, Ipsakis D, Triantafyllidis K, Lappas AA (2019) Cellulose conversion into lactic acid over supported HPA catalysts. *Green Chem* 21(22):6161–6178. <https://doi.org/10.1039/c9gc02622c>
- Palacio R, Torres S, Lopez D, Hernandez D (2018) Selective glycerol conversion to lactic acid on Co₃O₄/CeO₂

- catalysts. *Catal Today* 302:196–202. <https://doi.org/10.1016/j.cattod.2017.05.053>
- Peng D, Guo J, He J, Zhou X, Song K (2022) Separation of cellulose from *Pueraria Edulis* Pampan. Residue. *Chem Ind Prod* 42(1):79–86. <https://doi.org/10.3969/j.issn.0253-2417.2022.01.011>
- Pérez-Mayoral E, Calvino-Casilda V, Soriano E (2016) Metal-supported carbon-based materials: opportunities and challenges in the synthesis of valuable products. *Catal Sci Technol* 6(5):1265–1291. <https://doi.org/10.1039/c5cy01437a>
- Qureshi AS, Zhang J, da Costa Sousa L, Bao J (2017) Antibacterial peptide secreted by *Pediococcus acidilactici* enables efficient cellulose open l-lactic acid fermentation. *ACS Sustain Chem Eng* 5(10):9254–9262. <https://doi.org/10.1021/acssuschemeng.7b02212>
- Rahaman MS, Tulaphol S, Mills K, Molley A, Hossain MA, Lalvani S, Maihom T, Crocker M, Sathitsuksanoh N (2022) Aluminum-based metal-organic framework as water-tolerant lewis acid catalyst for selective dihydroxyacetone isomerization to lactic acid. *Chem-CatChem* 14(4):e202101756. <https://doi.org/10.1002/cctc.202101756>
- Sain M, Panthapulakkal S (2006) Bioprocess preparation of wheat straw fibers and their characterization. *Ind Crops Prod* 23(1):1–8. <https://doi.org/10.1016/j.indcrop.2005.01.006>
- Sangsiri P, Laosiripojana N, Daorattanachai P (2022) Synthesis of sulfonated carbon-based catalysts from organosolv lignin and methanesulfonic acid. *Renew Energy* 193:113–127. <https://doi.org/10.1016/j.renene.2022.05.012>
- Serrano-Ruiz JC, Luque R, Sepúlveda-Escribano A (2011) Transformations of biomass-derived platform molecules: from high added-value chemicals to fuels via aqueous-phase processing. *Chem Soc Rev* 40(11):5266–5281. <https://doi.org/10.1039/c1cs15131b>
- Shen Z, Kong L, Zhang W, Gu M, Xia M, Zhou X, Zhang Y (2019) Surface amino-functionalization of Sn-Beta zeolite catalyst for lactic acid production from glucose. *Rsc Adv* 9(33):18989–18995. <https://doi.org/10.1039/c9ra01264h>
- Suganuma S, Nakajima K, Kitano M, Kato H, Tamura A, Kondo H, Yanagawa S, Hayashi S, Hara M (2011) SO₃H-bearing mesoporous carbon with highly selective catalysis. *Microporous Mesoporous Mater* 143(2–3):443–450. <https://doi.org/10.1016/j.micromeso.2011.03.028>
- Sun XF, Xu F, Sun RC, Fowler P, Baird MS (2005) Characteristics of degraded cellulose obtained from steam-exploded wheat straw. *Carbohydr Res* 340(1):97–106. <https://doi.org/10.1016/j.carres.2004.10.022>
- Tang Z, Deng W, Wang Y, Zhu E, Wan X, Zhang Q, Wang Y (2014) Transformation of cellulose and its derived carbohydrates into formic and lactic acids catalyzed by vanadyl cations. *Chemoschem* 7(6):1557–1567. <https://doi.org/10.1002/cssc.201400150>
- Tanpichai S, Witayakran S, Srimarut Y, Woraprayote W, Malila Y (2019) Porosity, density and mechanical properties of the paper of steam exploded bamboo microfibers controlled by nanofibrillated cellulose. *J Mater Res Technol* 8(4):3612–3622. <https://doi.org/10.1016/j.jmrt.2019.05.024>
- Tarchoun AF, Trache D, Klapötke TM, Derradji M, Bessa W (2019) Ecofriendly isolation and characterization of microcrystalline cellulose from giant reed using various acidic media. *Cellulose* 26(13–14):7635–7651. <https://doi.org/10.1007/s10570-019-02672-x>
- Tong D, Chen X, Dong Y, Fang Z, Zhang H, Zhou C, Yu W (2022) Copper dispersed natural kaolinite as high-performance catalysts for the hydrolysis of cellulose in water. *Biomass Convers Biorefinery*. <https://doi.org/10.1007/s13399-022-02764-y>
- Wang F, Liu C, Dong W (2013) Highly efficient production of lactic acid from cellulose using lanthanide triflate catalysts. *Green Chem* 15(8):2091–2095. <https://doi.org/10.1039/c3gc40836a>
- Wang Y, Deng W, Wang B, Zhang Q, Wan X, Tang Z, Wang Y, Zhu C, Cao Z, Wang G, Wan H (2013) Chemical synthesis of lactic acid from cellulose catalysed by lead(II) ions in water. *Nat Commun* 4:2141. <https://doi.org/10.1038/ncomms3141>
- Wang Z, Mo C, Xu S, Chen S, Deng T, Zhu W, Wang H (2021) Ca(OH)₂ induced a controlled-release catalytic system for the efficient conversion of high-concentration glucose to lactic acid. *Mol Catal* 502:111406. <https://doi.org/10.1016/j.mcat.2021.111406>
- Wattanaphawong P, Reubroycharoen P, Yamaguchi A (2017) Conversion of cellulose into lactic acid using zirconium oxide catalysts. *RSC Adv* 7(30):18561–18568. <https://doi.org/10.1039/c6ra28568f>
- Wei C, Liu G, Xie Y, Sun Z, Liu C, Song F, Cui H (2022) Cellulose dissolution and conversion into 5-hydroxymethylfurfural in mixed molten salt hydrate. *Cellulose* 30(2):801–813. <https://doi.org/10.1007/s10570-022-04967-y>
- Wu T, Li N, Pan X, Chen S (2020) Homogenous hydrolysis of cellulose to glucose in an inorganic ionic liquid catalyzed by zeolites. *Cellulose* 27(16):9201–9215. <https://doi.org/10.1007/s10570-020-03411-3>
- Xiao Y, Liao S, Xu S, Li J, Lu Z, Hu C (2022) Selective transformation of typical sugars to lactic acid catalyzed by dealuminated ZSM-5 supported erbium. *Renew Energy* 187:551–560. <https://doi.org/10.1016/j.renene.2022.01.100>
- Xu J, Zhang H, Zhao Y, Yu B, Chen S, Li Y, Hao L, Liu Z (2013) Selective oxidation of glycerol to lactic acid under acidic conditions using AuPd/TiO₂ catalyst. *Green Chem* 15(6):1520–1525. <https://doi.org/10.1039/c3gc40314a>
- Xu H, Ye X, Shi X, Zhong H, He D, Jin B, Jin F (2022) ZnO as a simple and facile catalyst for acid-base coordination transformation of biomass-based monosaccharides into lactic acid. *Mol Catal* 522:112241. <https://doi.org/10.1016/j.mcat.2022.112241>
- Yang X, Yang L, Fan W, Lin H (2016) Effect of redox properties of LaCoO₃ perovskite catalyst on production of lactic acid from cellulosic biomass. *Catal Today* 269:56–64. <https://doi.org/10.1016/j.cattod.2015.12.003>
- Yang H, Zhou Y, Tong D, Yang M, Fang K, Zhou C, Yu W (2020) Catalytic conversion of cellulose to reducing sugars over clay-based solid acid catalyst supported nano-sized SO₄²⁻-ZrO₂. *Appl Clay Sci* 185:105376. <https://doi.org/10.1016/j.clay.2019.105376>
- Ye J, Chen C, Zheng Y, Zhou D, Liu Y, Chen D, Ni L, Xu G, Wang F (2021) Efficient conversion of cellulose to lactic

- acid over yttrium modified siliceous Beta zeolites. *Appl Catal A-gen* 619:118133. <https://doi.org/10.1016/j.apcata.2021.118133>
- Yue X, He J, Xu Y, Yang M, Xu Y (2019) A novel method for preparing microcrystalline cellulose from bleached chemical pulp using transition metal ions enhanced high temperature liquid water process. *Carbohydr Polym* 208:115–123. <https://doi.org/10.1016/j.carbpol.2018.12.072>
- Zhang S, Jin F, Hu J, Huo Z (2011) Improvement of lactic acid production from cellulose with the addition of Zn/Ni/C under alkaline hydrothermal conditions. *Bioresour Technol* 102(2):1998–2003. <https://doi.org/10.1016/j.biortech.2010.09.049>
- Zhang H, Liu W, Cao D, Cheng D (2022) Carbon-based material-supported single-atom catalysts for energy conversion. *iScience* 25(6):104367. <https://doi.org/10.1016/j.isci.2022.104367>
- Zhao B, Yue X, Li H, Li J, Liu C-L, Xu C, Dong W-S (2018) Lanthanum-modified phosphomolybdic acid as an efficient catalyst for the conversion of fructose to lactic acid. *React Kinet Mech Catal* 125(1):55–69. <https://doi.org/10.1007/s11144-018-1416-y>
- Zhao X, Zhou Z, Luo H, Zhang Y, Liu W, Miao G, Zhu L, Kong L, Li S, Sun Y (2021) γ -Valerolactone-introduced controlled-isomerization of glucose for lactic acid production over an Sn-Beta catalyst. *Green Chem* 23(7):2634–2639. <https://doi.org/10.1039/d1gc00378j>

Publisher's Note Springer Nature remains neutral with regard to jurisdictional claims in published maps and institutional affiliations.

Springer Nature or its licensor (e.g. a society or other partner) holds exclusive rights to this article under a publishing agreement with the author(s) or other rightsholder(s); author self-archiving of the accepted manuscript version of this article is solely governed by the terms of such publishing agreement and applicable law.